Clin. Lab. 2027;73:XXX-XXX
©Copyright

ORIGINAL ARTICLE

Distinct STM Subsets Mediate RA Inflammation and Remission via NF-κB/JAK1/STAT3 Signaling

YingYi Wu [1], Yan Bian [2], Jing Fei [1], Yang Huang [1]

[1] *Department of Rheumatology, Affiliated Hospital of Jiangnan University, Wuxi City, Jiangsu Province, China*
[2] *Department of Nephrology, Jiangsu Province Hospital, Nanjing City, Jiangsu Province, China*

ABSTRACT

Background: **Rheumatoid arthritis (RA) represents a chronic autoimmune condition wherein synovial tissue macrophages (STMs) play a crucial role in inflammation. However, the precise functions and regulatory mechanisms of specific STM subsets during the progression and resolution of inflammation remain poorly defined. This study aimed to delineate the roles of different STM subpopulations across the inflammatory and remission stages of RA, and to evaluate their role in disease progression through the nuclear factor kappa B (NF-κB) and Janus kinase 1/Signal Transducer and Activator of Transcription 3 (JAK1/STAT3) signaling pathways.**
Methods: **A total of 110 RA patients and 20 healthy controls were recruited. Flow cytometry was employed to examine CD163, CD206, and Mer tyrosine kinase (MerTK) expression in synovial tissue, allowing identification of STM subsets based on surface markers. An *in vitro* lipopolysaccharide (LPS) stimulation assay was performed to compare secretion of pro-inflammatory cytokines (interleukin-1β [IL-1β], IL-6, tumor necrosis factor-α [TNF-α]) and the pro-resolving mediator Resolvin D1 (RvD1) between $MerTK^+CD206^+$ and $MerTK^-CD206^-$ STMs. Western blot analysis was used to detect proteins associated with the NF-κB and JAK1/STAT3 pathways.**
Results: **Patients in clinical remission exhibited notably elevated proportions of $MerTK^+CD206^+$, $CD163^+CD206^+$, and $MerTK^+CD163^+$ STMs within synovial tissue relative to those with active RA. The frequency of $MerTK^+CD206^+$ STMs showed a negative correlation with the Disease Activity Score in 28 joints (DAS28). *In vitro*, following LPS challenge, $MerTK^+CD206^+$ STMs released significantly lower amounts of pro-inflammatory cytokines and uniquely generated RvD1, whereas $MerTK^-CD206^-$ STMs produced higher pro-inflammatory cytokine levels. Western blot analyses indicated that phosphorylation levels of NF-κB (p-NF-κB), JAK1 (p-JAK1), and STAT3 (p-STAT3) were markedly reduced in $MerTK^+CD206^+$ compared to $MerTK^-CD206^-$ STMs.**
Conclusions: **The $MerTK^+CD206^+$ STM subset expands during RA remission. Through suppression of NF-κB and JAK1/STAT3 signaling pathways, these cells curtail pro-inflammatory cytokine release and foster inflammation resolution, thereby playing an instrumental role in attenuating inflammation and supporting tissue repair in RA.**
(Clin. Lab. 2027;73:xx-xx. DOI: 10.7754/Clin.Lab.2026.260223)

Correspondence:
Yang Huang
Department of Rheumatology
Affiliated Hospital of Jiangnan University
No. 1000, Hefeng Road
Binhu District
Wuxi City
Jiangsu Province, 214100
China
Email: yanghu881@outlook.com

Manuscript accepted September 14, 2026

KEYWORDS

rheumatoid arthritis, synovial tissue macrophages, MerTK, CD206, NF-κB signaling pathway, JAK1/STAT3 signaling pathway, inflammation resolution

LIST OF ABBREVIATIONS

RA - Rheumatoid Arthritis
STM - Synovial Tissue Macrophage
MerTK - Mer Tyrosine Kinase
NF-κB - Nuclear Factor Kappa B

JAK1 - Janus Kinase 1
STAT3 - Signal Transducer and Activator of Transcription 3
DAS28 - Disease Activity Score in 28 Joints
LPS - Lipopolysaccharide
IL-1β - Interleukin-1 Beta
IL-6 - Interleukin-6
TNF-α - Tumor Necrosis Factor-Alpha
RvD1 - Resolvin D1
SPM - Specialized Pro-Resolving Mediator
MTX - Methotrexate
ELISA - Enzyme-Linked Immunosorbent Assay
FACS - Fluorescence-Activated Cell Sorting
PBS - Phosphate-Buffered Saline
FBS - Fetal Bovine Serum
RIPA - Radioimmunoprecipitation Assay
SDS-PAGE - Sodium Dodecyl Sulfate-Polyacrylamide Gel Electrophoresis
PVDF - Polyvinylidene Difluoride
GAPDH - Glyceraldehyde 3-Phosphate Dehydrogenase
ACPA - Anti-Citrullinated Protein Antibodies
RF/IgM-RF - Rheumatoid Factor/Immunoglobulin M Rheumatoid Factor
IgA-RF - Immunoglobulin A Rheumatoid Factor
ESR - Erythrocyte Sedimentation Rate
CRP - C-Reactive Protein
BMI - Body Mass Index
ACL - Anterior Cruciate Ligament
TLR4 - Toll-Like Receptor 4
TAM - Tyro3, Axl, MerTK (Receptor Family)
Gas6 - Growth Arrest-Specific 6
SD - Standard Deviation
CI - Confidence Interval
p-NF-κB - Phosphorylated NF-κB
p-JAK1 - Phosphorylated JAK1
p-STAT3 - Phosphorylated STAT3
TBST - Tris-buffered Saline with Tween-20

INTRODUCTION

Rheumatoid arthritis (RA) is a progressive autoimmune disease characterized by synovial inflammation, hyperplasia, and subsequent cartilage and bone destruction [1]. Affecting about 1% of the global population, RA leads to impaired mobility, reduced quality of life, and increased risk of comorbidities such as cardiovascular disease, diabetes, and obesity [2,3]. Many patients respond inadequately to existing treatments, and clinical outcomes, such as progression to erosive disease or favorable therapeutic response, remain challenging to predict [4]. Hence, clarifying the exact pathogenic mechanisms within inflamed joints is vital for developing new therapeutic approaches.

In healthy synovium, resident synovial tissue macrophages (STMs) constitute the major immune cell population, outnumbering dendritic cells and lymphocytes [5]. During active RA, which features mixed myeloid and lymphoid synovitis, the synovial space becomes heavily infiltrated with leukocytes. This includes an increase in pro-inflammatory macrophages, thought to arise mainly from blood monocytes recruited by local chemokines [6]. These cells are key sources of pathogenic tumor necrosis factor (TNF), a principal driver of inflammation [7,8]. Interestingly, while overt synovitis largely resolves during remission, a population of STMs remains within the synovial lining [9]. It is important to determine whether these residual macrophages resemble those in healthy tissue. Their persistence in both healthy and remission states implies that specific STM subsets may help maintain synovial homeostasis [10,11]. Single-cell transcriptomic profiling by Alivernini et al. identified a Mer tyrosine kinase $(MerTK)^{+}CD206^{+}$ synovial macrophage subset associated with disease remission in RA, providing a foundational transcriptional landscape of macrophage heterogeneity in inflamed synovium [12]. However, protein-level validation, functional characterization, and clinical correlation in independent cohorts have yet to be fully elucidated.

Considerable evidence points to dysregulated nuclear factor kappa B (NF-κB) activation in the pathogenesis of several autoimmune diseases, including RA [13,14]. NF-κB encompasses a family of inducible transcription factors that control expression of many genes essential for immune and inflammatory responses [15]. In RA, aberrant NF-κB signaling sustains chronic inflammation and directly promotes joint damage [16].

The Janus Kinase (JAK)/Signal Transducer and Activator of Transcription (STAT) pathway is another critical signaling axis in RA, mediating pivotal immune and inflammatory events within the synovium [17]. Cytokines like tumor necrosis factor-α (TNF-α) and interleukin-6 (IL-6) can activate the Janus kinase 1/Signal Transducer and Activator of Transcription 3 (JAK1/STAT3) signaling pathways, thereby amplifying inflammatory and immune responses [18,19].

The current study was undertaken to examine the distinct roles of STM subsets during active inflammation and remission in RA, and to assess their contribution to disease progression through modulation of the NF-κB and JAK1/STAT3 signaling pathways.

MATERIALS AND METHODS

Patient recruitment, arthroscopy, and sample collection

The study protocol was approved by the Institutional Ethics Committee of Affiliated Hospital of Jiangnan University, and written informed consent was obtained from all participants. The cohort consisted of patients diagnosed with RA under care at the institution, all meeting the 2010 American College of Rheumatology revised classification criteria for RA [20]. Synovial tissue from RA patients was obtained via ultrasound-guided needle biopsy of the knee.

Healthy control subjects were recruited from individuals undergoing elective knee arthroscopy for anterior cruci-

ate ligament (ACL) reconstruction. Inclusion criteria for controls included: 1) no clinical history or physical exam findings indicating arthritis; 2) absence of cartilage damage or synovitis during arthroscopy; and 3) histological verification of normal synovial architecture without inflammatory infiltrates.

Synovial tissue dissociation

Synovial biopsy specimens acquired during arthroscopy were processed into single-cell suspensions. Mechanical and enzymatic digestion was carried out using a GentleMACS™ Dissociator with a human Tumor Dissociation Kit (Miltenyi Biotec, Bergisch Gladbach, Germany) per the manufacturer's protocol. The resulting cell suspension was filtered through a 70 µm sterile cell strainer to eliminate tissue debris.

Flow cytometry

For flow cytometric analysis, synovial tissue-derived cells were washed and resuspended in phosphate-buffered saline (PBS). Cell viability was evaluated by staining with the LIVE/DEAD™ Fixable Red Dead Cell Stain Kit (Thermo Fisher Scientific, Waltham, MA, USA) for 30 minutes at 4 °C in the dark. Unless otherwise specified, all centrifugation steps were performed at 400 × g for 5 minutes at 4 °C.

After LIVE/DEAD staining, cells were centrifuged and the pellet was resuspended in 100 µL of fluorescence-activated cell sorting (FACS) buffer, consisting of Dulbecco's PBS (without Mg^{2+} and Ca^{2+}; Sigma-Aldrich, St. Louis, MO, USA) supplemented with 1% heat-inactivated fetal bovine serum (FBS; Gibco, Grand Island, NY, USA), 0.05% sodium azide (Sigma-Aldrich), and 1 mM EDTA, pH 7.4 - 7.6.

To reduce nonspecific antibody binding, samples were pre-incubated with 5 µL of Human TruStain FcX™ Fc receptor blocking solution (BioLegend, San Diego, CA, USA, Cat# 422302) for 10 minutes at 4 °C. A cocktail of fluorochrome-conjugated monoclonal antibodies was then added for surface staining; all antibodies were pre-titrated to determine optimal working concentrations. The following antibodies were used: BV421 anti-human CD11b (Clone: ICRF44, mouse IgG1, κ; BD Biosciences, Franklin Lakes, NJ, USA, Cat# 562632), BV605 anti-human CD64 (Clone MD22, mouse IgG1, κ; BD Biosciences, Cat# 569721), RB705 anti-human CD163 (Clone GHI/61, mouse IgG1, κ; BD Biosciences, Cat# 570688), BV510 anti-human CD206 (Clone 19.2, mouse IgG1, κ; BD Biosciences, Cat# 569618), and PE anti-human MerTK (Clone CC3-47, mouse IgG1, κ; BD Biosciences, Cat# 571779). Samples were mixed gently and incubated at 4 °C for 30 minutes in the dark.

Following staining, cells were washed twice with FACS buffer and centrifuged as described above. The final cell pellet was resuspended in 250 µL of FACS buffer and filtered through a 40 µm sterile cell strainer immediately before data acquisition to remove cell aggregates.

Data acquisition was performed on a BD LSRFortessa™ flow cytometer (BD Biosciences). Compensation calibration was performed prior to each experiment as follows: i) for all fluorochrome-conjugated mouse IgGκ antibodies, compensation was set up using BD CompBeads™ Anti-Mouse Ig, κ (BD Biosciences, Cat# 552843) according to the manufacturer's instructions; ii) for the amine-reactive LIVE/DEAD dye, compensation was calibrated using a single-stained cell control prepared by mixing equal numbers of heat-killed (56 °C, 30 minutes) and live synovial cells prior to viability staining.

Data analysis was performed with FlowJo v10 software (Treestar Inc., USA). The gating strategy was as follows: cells were first gated on forward scatter area (FSC-A) versus side scatter area (SSC-A) to select the total cell population, followed by FSC-A versus FSC-height (FSC-H) to exclude doublets. Live cells were then selected based on the negative signal of the viability dye. Within the live cell population, STMs were identified as $CD11b^{+}CD64^{+}$ cells. The expression of CD163, CD206, and MerTK on STMs was further analyzed to define distinct subsets.

***In vitro* stimulation of sorted STMs**

For parallel LPS stimulation and functional assays, $MerTK^{+}CD206^{+}$ and $MerTK^{-}CD206^{-}$ STM subsets were sorted from synovial tissues of patients with active RA and those in clinical remission, respectively. After fluorescence-activated cell sorting (FACS), $MerTK^{+}CD206^{+}$ and $MerTK^{-}CD206^{-}$ STM subsets were collected into complete culture medium. Cells were seeded onto 96-well flat-bottom plates pre-coated with bovine collagen I (Sigma-Aldrich) at 1:300 dilution. Coating involved adding collagen solution to wells and incubating for 2 hours at 37 °C under 5% CO_2. Wells were then washed twice with sterile PBS. Sorted STMs were plated at 1×10^5 cells per well and stimulated with 10 ng/mL lipopolysaccharide (LPS; Sigma-Aldrich, Cat# L6529) for 24 hours [12].

Enzyme-linked immunosorbent assay (ELISA)

Post-stimulation, culture supernatants were collected and clarified by centrifugation. Secreted levels of interleukin-1β (IL-1β; Cayman Chemical, Ann Arbor, MI, USA, Cat# 583311), IL-6 (Cayman Chemical, Cat# 501030), TNF-α (R&D Systems, Minneapolis, MN, USA, Cat# DTA00C), and Resolvin D1 (RvD1; Cayman Chemical, Cat# 500380), a specialized pro-resolving mediator (SPM), were measured using commercial ELISA kits according to the manufacturer's instructions. All cytokine and specialized pro-resolving mediator concentrations were expressed in picograms per milliliter (pg/mL).

Western blot

Total cellular protein was extracted using radioimmunoprecipitation assay (RIPA) lysis buffer containing 1% phenylmethylsulfonyl fluoride (Beyotime Biotechnology, Shanghai, China). Protein concentrations were determined with a bicinchoninic acid assay kit (Beyotime

Table 1. Demographic and clinical characteristics of study participants.

Characteristics		Healthy control (n = 20)	Active RA (n = 75)		Remission RA (n = 35)
			Naive RA (n = 45)	Resistant RA (n = 30)	
Age, years (mean ± SD)		55.69 ± 10.45	54.58 ± 15.57	57.81 ± 8.72	57.00 ± 16.31
Gender n (%)	male	8	5	4	7
	female	12	40	26	28
BMI, kg/m^2 (mean ± SD)		25.72 ± 5.38	25.64 ± 5.63	26.29 ± 5.74	24.57 ± 4.61
Disease duration, years (mean ± SD)			1.56 ± 1.60	4.23 ± 2.86	5.72 ± 3.15
DAS28 value, (mean ± SD)			5.27 ± 0.92	5.45 ± 0.93	1.86 ± 0.49
Total RF positivity, n (%)			30	22	24
ACPA positivity, n (%)			27	20	20
IgM-RF positivity, n (%)			26	18	18
IgA-RF positivity, n (%)			18	17	15
ESR, mm/1st hour (mean ± SD)			42.07 ± 26.13	45.19 ± 27.84	14.53 ± 10.66
CRP, mg/L (mean ± SD)			19.34 ± 13.35	24.59 ± 21.91	3.01 ± 4.02

SD: standard deviation, BMI: body mass index, DAS28: Disease Activity Score in 28 joints, ACPA: anti-citrullinated protein antibodies, IgM-RF: immunoglobulin M rheumatoid factor, IgA-RF: immunoglobulin A rheumatoid factor, ESR: erythrocyte sedimentation rate, CRP: C-reactive protein. Total RF positivity indicates positivity for either IgM-RF or IgA-RF.

Table 2. Correlation between STM subset frequencies and DAS28 in active RA patients.

	DAS28 value		
	r	95% CI	p-value
MerTK$^+$CD206$^+$ cells (%)	-0.4919	-0.6506 to -0.2920	< 0.0001
CD163$^+$CD206$^+$ cells (%)	-0.2918	-0.4917 to -0.06259	0.0111
MerTK$^+$CD163$^+$ cells (%)	-0.2446	-0.4523 to -0.01190	0.0344

STM: synovial tissue macrophage, DAS28: disease activity score in 28 joints, CI: confidence interval, RA: rheumatoid arthritis, MerTK: Mer tyrosine kinase, CD206: cluster of differentiation 206 (macrophage mannose receptor), CD163: cluster of differentiation 163 (scavenger receptor).

Table 3. Correlation between STM subset frequencies and DAS28 in remission RA patients.

	DAS28 value		
	r	95% CI	p-value
MerTK$^+$CD206$^+$ cells (%)	-0.5629	-0.7589 to -0.2732	0.0004
CD163$^+$CD206$^+$ cells (%)	-0.3625	-0.6270 to -0.02300	0.0324
MerTK$^+$CD163$^+$ cells (%)	-0.3458	-0.6153 to -0.004000	0.0418

STM: synovial tissue macrophage, DAS28: disease activity score in 28 joints, CI: confidence interval, RA: rheumatoid arthritis, MerTK: Mer tyrosine kinase, CD206: cluster of differentiation 206 (macrophage mannose receptor), CD163: cluster of differentiation 163 (scavenger receptor).

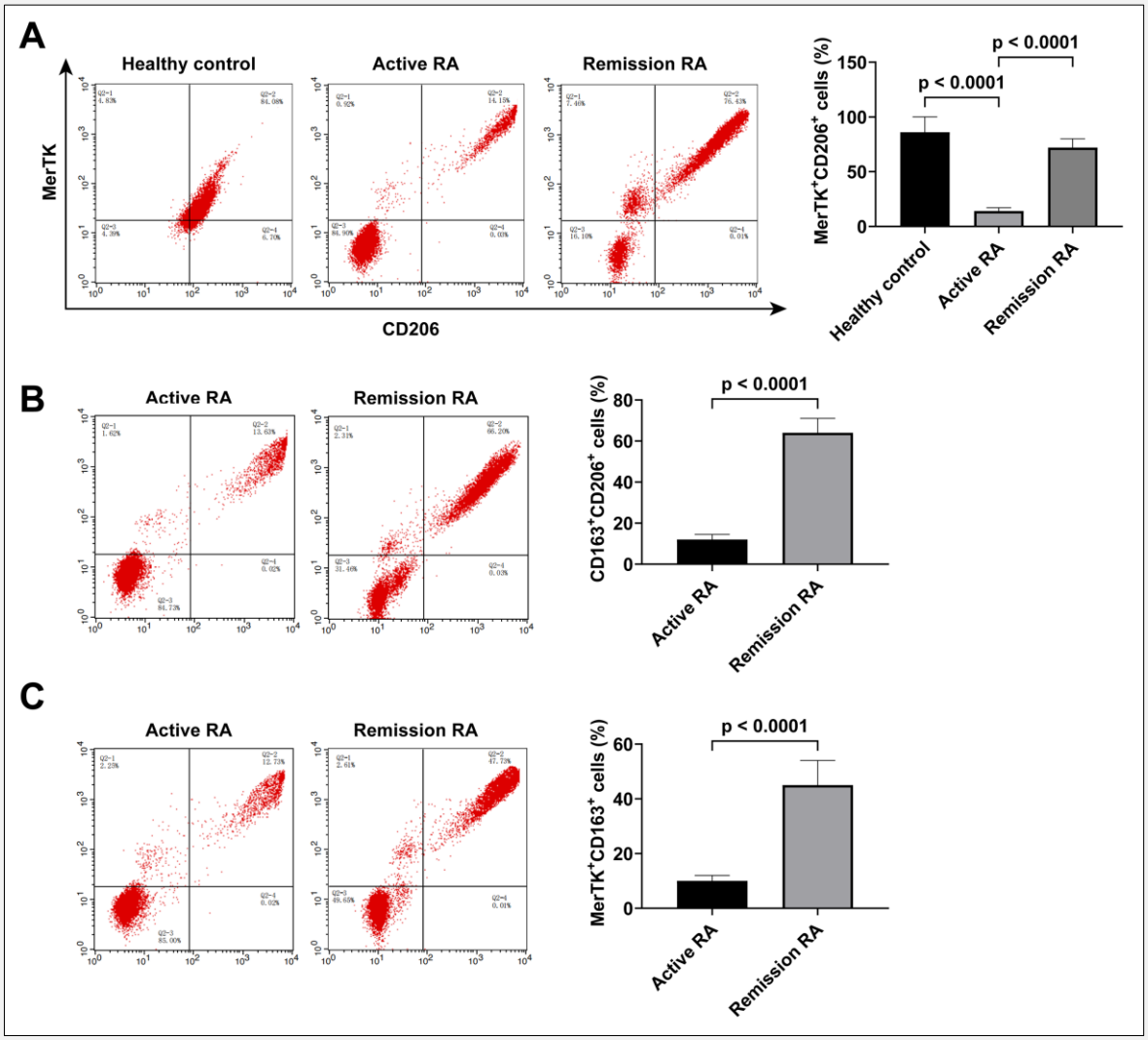


Figure 1. Increased proportion of MerTK$^+$CD206$^+$ macrophages in synovial tissue of RA patients in remission.

A: Flow cytometric analysis of the proportion of MerTK$^+$CD206$^+$ STMs; Kruskal-Wallis H test. B: Flow cytometric analysis of the proportion of CD163$^+$CD206$^+$ STMs; Mann-Whitney U test. C: Flow cytometric analysis of the proportion of MerTK$^+$CD163$^+$ STMs; Mann-Whitney U test. The data are presented as mean ± standard deviation (SD). n = 20 for healthy controls, n = 75 for active RA, n = 35 for remission RA. * p < 0.05, ** p < 0.01, *** p < 0.001, **** p < 0.0001.

Biotechnology). Equal protein amounts from each sample were separated by 12% sodium dodecyl sulfate-polyacrylamide gel electrophoresis (SDS-PAGE) and transferred to polyvinylidene difluoride membranes (Millipore, Burlington, MA, USA). Membranes were blocked with 5% bovine serum albumin (BSA) in tris-buffered saline with Tween-20 (TBST) for 90 minutes at room temperature, then incubated overnight at 4 °C with primary antibodies. Antibodies used (all Cell Signaling Technology, Danvers, MA, USA, 1:1000 dilution) included: anti-NF-κB (Cat# 8242), anti-phospho-NF-κB (p-NF-κB; Cat# 3033), anti-JAK1 (Cat# 3344), anti-phospho-JAK1 (p-JAK1; Cat# 74129), anti-STAT3 (Cat# 12640), anti-phospho-STAT3 (p-STAT3; Cat# 9145), and anti-glyceraldehyde 3-phosphate dehydrogenase (GAPDH; Cat# 5174). Following thorough washing, membranes were incubated with appropriate horseradish peroxidase-conjugated secondary antibodies for 90 minutes at room temperature. Protein bands were visualized using enhanced chemiluminescence substrate (Millipore). All western blot experiments were performed independently in triplicate (n = 3), and protein levels were normalized to GAPDH as a loading control.

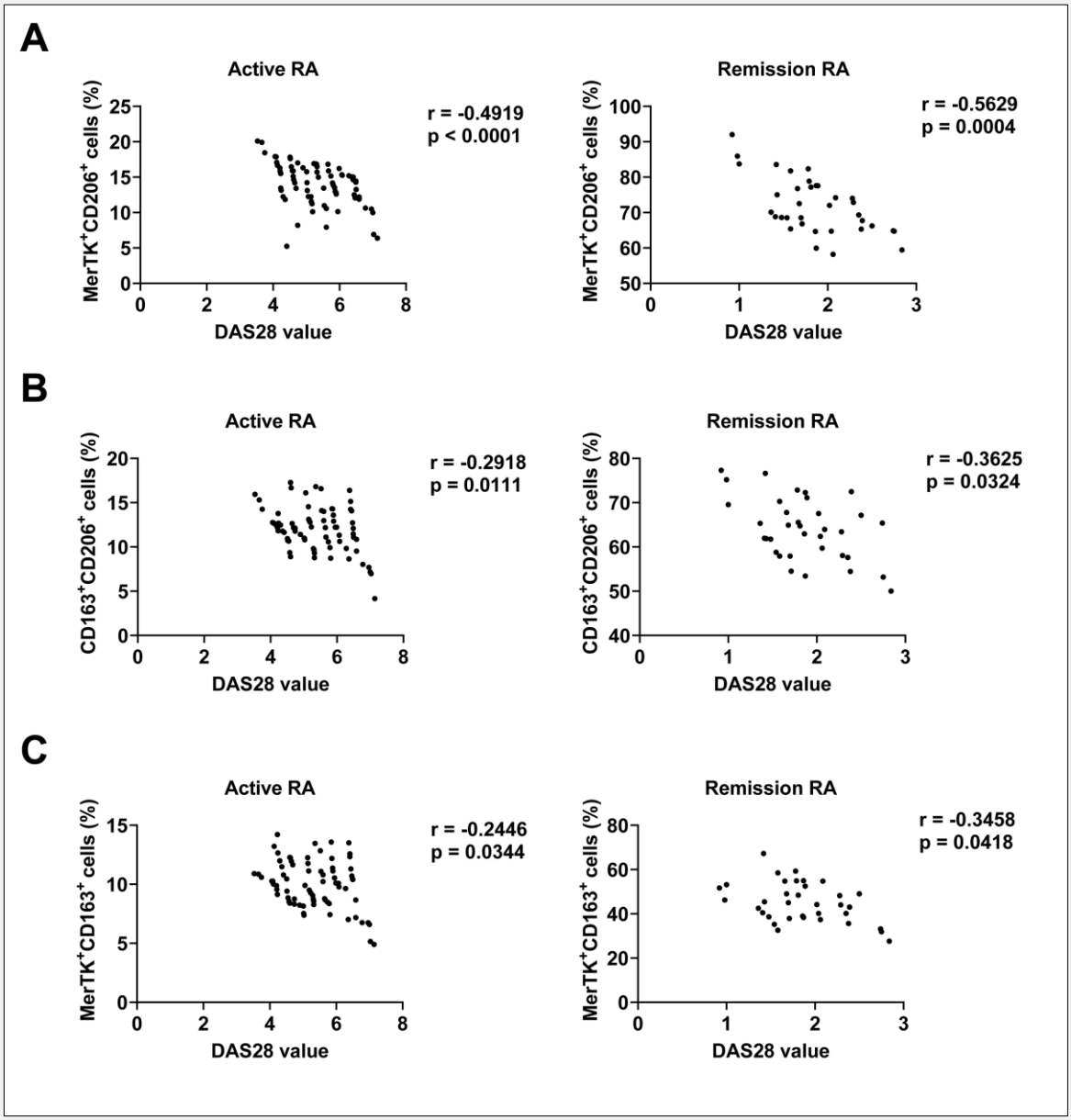


Figure 2. Proportion of MerTK$^+$CD206$^+$ macrophages in synovial tissue is inversely correlated with RA disease activity score.

A: Spearman's correlation analysis between the proportion of MerTK$^+$CD206$^+$ STMs and the DAS28 score. B: Spearman's correlation analysis between the proportion of CD163$^+$CD206$^+$ STMs and the DAS28 score. C: Spearman's correlation analysis between the proportion of MerTK$^+$CD163$^+$ STMs and the DAS28 score. n = 75 for active RA, n = 35 for remission RA.

Statistical analysis

Statistical analyses were performed using GraphPad Prism software (version 10.0; GraphPad Software, Boston, MA, USA). Normality of data distribution was assessed via the Shapiro-Wilk test. Sample size estimation was performed using G*Power 3.1 software, with the difference in the proportion of synovial MerTK$^+$CD206$^+$ STM subsets between active and remission RA patients designated as the primary endpoint. Based on preliminary experimental results and published data from similar studies, a two-sided significance level of $\alpha = 0.05$ and a statistical power of $1 - \beta = 0.80$ were used. A min-

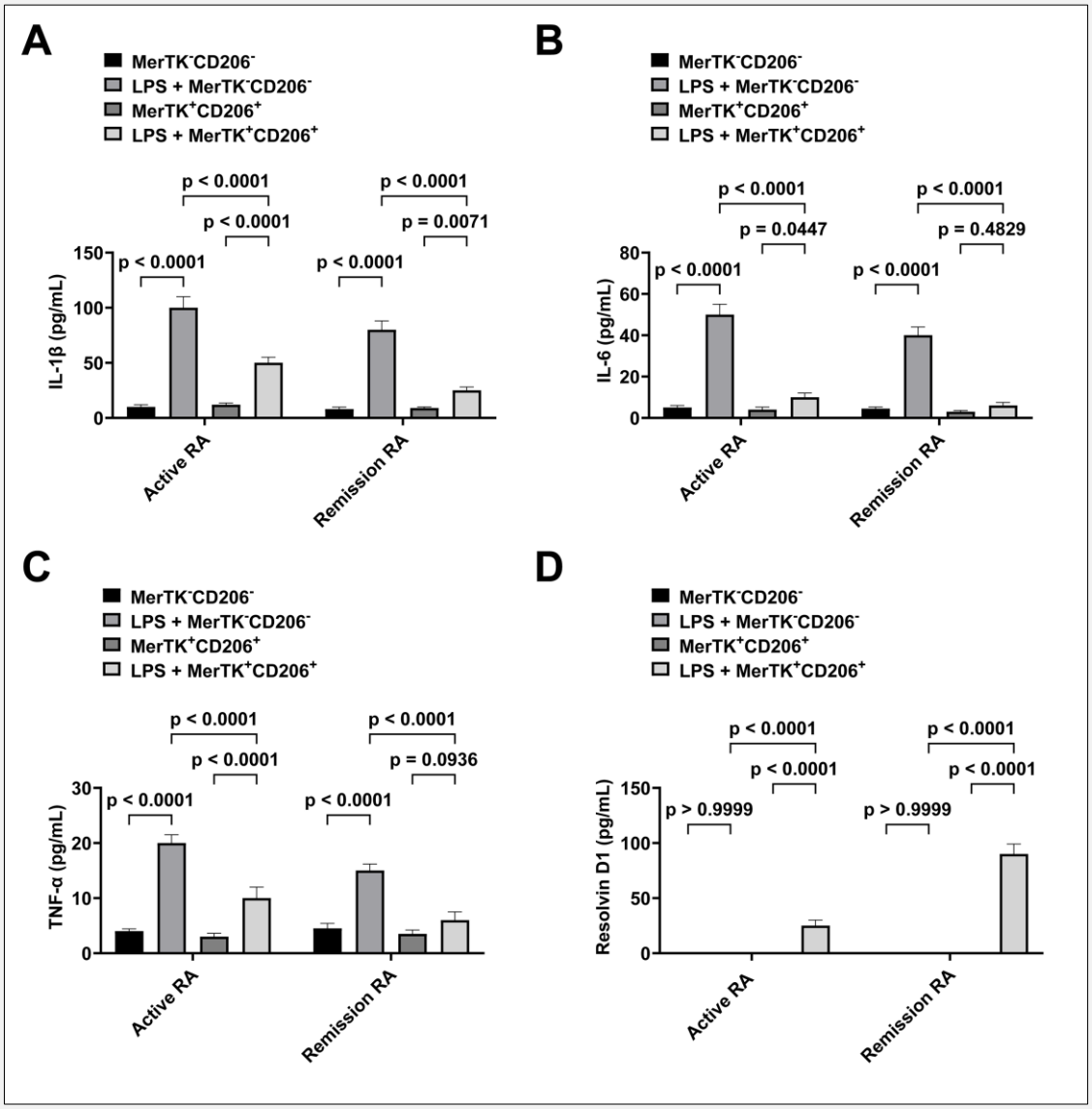


Figure 3. MerTK$^+$CD206$^+$ macrophages promote inflammation resolution.

A - C: Measurement of pro-inflammatory cytokines (IL-1β, IL-6, TNF-α); one-way ANOVA. D: Measurement of the lipid mediator RvD1; one-way ANOVA. The data are presented as mean ± SD. n = 3. * p < 0.05, ** p < 0.01, *** p < 0.001, **** p < 0.0001.

imum of 29 participants per group was calculated using the two-independent-samples *t*-test. Ultimately, 75 patients with active RA and 35 patients with clinical remission RA were enrolled in this study. The actual sample sizes substantially exceeded the calculated minimum requirements for both groups, ensuring adequate statistical power. For comparisons involving three or more groups, one-way analysis of variance (ANOVA) was applied for normally distributed parametric data. When the overall test reached statistical significance ($p < 0.05$), post-hoc pairwise comparisons were performed and p-values were adjusted using the Benjamini-Hochberg false discovery rate (FDR) method. For data not normally distributed, the Kruskal-Wallis H test was used for overall group comparison, followed by Dunn's post-hoc test with FDR adjustment for pairwise comparisons. For comparisons between two groups, Student's *t*-test was used for parametric data and the Mann-Whitney U test for non-parametric data. All raw p-values derived from multiple endpoint measurements were cor-

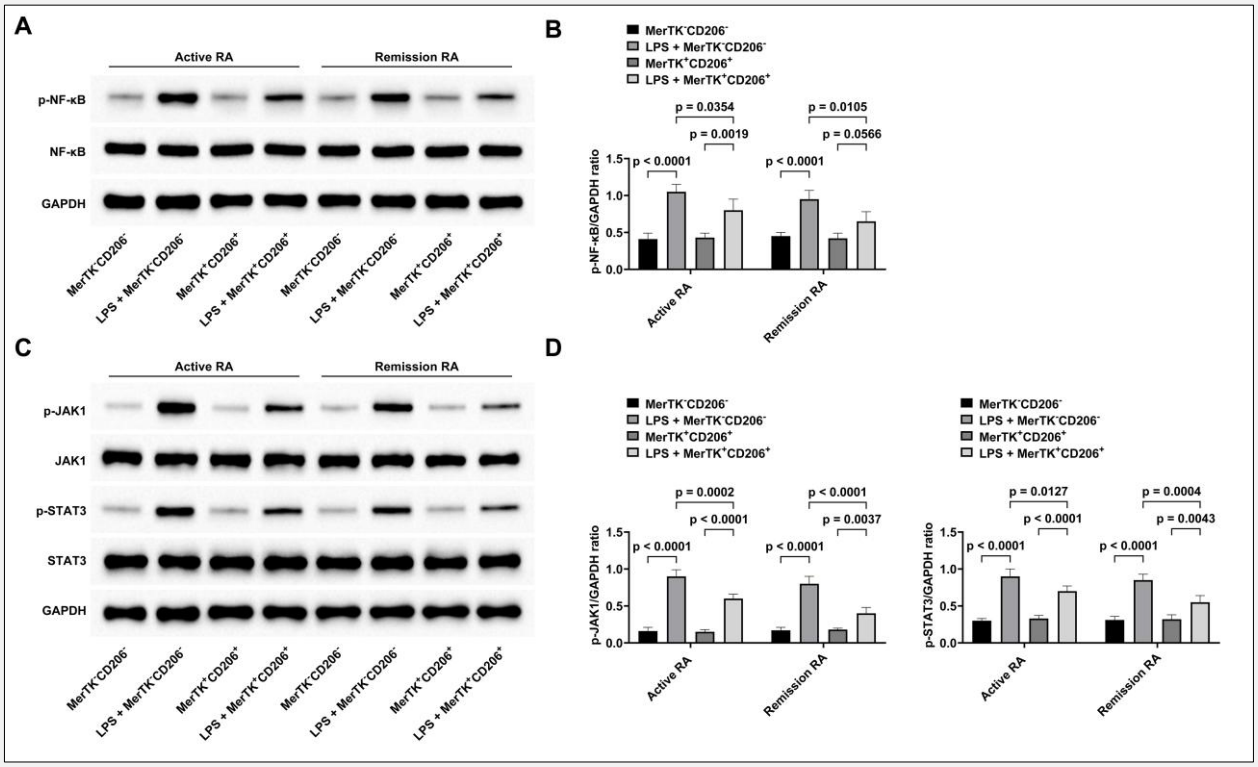


Figure 4. MerTK$^+$CD206$^+$ macrophages suppress the activation of NF-κB and JAK1/STAT3 signaling pathways.

A - D: Western blot analysis of proteins related to the NF-κB and JAK1/STAT3 signaling pathways; one-way ANOVA. The data are presented as mean ± SD. n = 3. * p < 0.05, ** p < 0.01, *** p < 0.001, **** p < 0.0001.

rected using the Benjamini-Hochberg FDR method to account for multiple testing. Correlations between frequencies of STM subsets (MerTK$^+$CD206$^+$, CD163$^+$ CD206$^+$, and MerTK$^+$CD163$^+$) and the Disease Activity Score in 28 joints (DAS28) were evaluated using Spearman's rank correlation coefficient. A two-tailed p-value < 0.05 was considered statistically significant. No artificial intelligence-assisted technologies were used in the production of this manuscript.

RESULTS

Demographic and clinical characteristics of RA patients

The study included 110 RA patients and 20 healthy controls; demographic and clinical characteristics are presented in Table 1. Among RA patients, 75 had active disease (including 45 treatment-naïve and 30 with inadequate response to methotrexate [MTX]), while 35 had achieved sustained clinical remission (≥ 6 months) following treatment with MTX plus a TNF inhibitor.

Increased proportion of MerTK$^+$CD206$^+$ macrophages in synovial tissue of RA patients in remission

Flow cytometric analysis of CD163, CD206, and MerTK expression identified distinct STM subsets. The MerTK$^+$CD206$^+$ phenotype predominated in healthy control samples (Figure 1A). Notably, the proportion of MerTK$^+$CD206$^+$ STMs was significantly higher in synovial tissue from RA patients in clinical remission compared to active disease (Figure 1A). Moreover, frequencies of CD163$^+$CD206$^+$ and MerTK$^+$CD163$^+$ subsets were also elevated in the remission group relative to active RA (Figure 1B, C).

Proportion of MerTK$^+$CD206$^+$ macrophages in synovial tissue is inversely correlated with RA disease activity score

Statistical analysis further indicated a significant inverse relationship between disease activity and specific STM phenotypes. Negative correlations were observed between DAS28 scores and the proportions of MerTK$^+$ CD206$^+$, CD163$^+$CD206$^+$, and MerTK$^+$CD163$^+$ macrophages (Figure 2A - C, Tables 2 and 3).

MerTK$^+$CD206$^+$ macrophages promote inflammation resolution

To characterize the functional properties of MerTK$^+$ CD206$^+$ and MerTK$^-$CD206$^-$ STM subsets, their response to inflammatory stimulation was tested *in vitro*. Cells were treated with LPS, a toll-like receptor 4 (TLR4) ligand known to induce strong pro-inflammatory cytokine production. Analysis of culture supernatants revealed that MerTK$^-$CD206$^-$ STMs secreted markedly higher levels of IL-1β, IL-6, and TNF-α after LPS stimulation compared to MerTK$^+$CD206$^+$ STMs (Figure 3A - C). In contrast, synthesis of the specialized pro-resolving lipid mediator RvD1 occurred exclusively in the MerTK$^+$CD206$^+$ subset. Notably, MerTK$^+$CD206$^+$ STMs isolated from RA patients in clinical remission released significantly greater quantities of RvD1 (Figure 3D). Together, these functional data indicate that the MerTK$^+$CD206$^+$ macrophage subset possesses a distinct capacity to promote inflammation resolution.

MerTK$^+$CD206$^+$ macrophages suppress the activation of NF-κB and JAK1/STAT3 signaling pathways

To explore the mechanisms underlying the pro-resolving phenotype of MerTK$^+$CD206$^+$ STMs, the activation status of key inflammatory signaling pathways was examined. Western blot analysis measured phosphorylation levels of proteins in the NF-κB and JAK1/STAT3 signaling pathways. Upon LPS challenge, MerTK$^-$ CD206$^-$ STMs exhibited significantly greater activation of these pathways, as evidenced by substantially higher levels of p-NF-κB, p-JAK1, and p-STAT3 relative to MerTK$^+$CD206$^+$ STMs (Figure 4A - D). This suggests that the attenuated inflammatory response in MerTK$^+$ CD206$^+$ macrophages correlates with reduced activation of NF-κB and JAK1/STAT3 signaling pathways.

DISCUSSION

RA is a chronic autoimmune disorder mainly affecting synovial tissue, driving inflammation, hyperplasia, and progressive joint damage [21,22]. Although modern treatments, including biologics and targeted small molecules, have improved outcomes for many, a substantial proportion of patients show incomplete responses or fail to sustain long-term remission [23]. Therefore, clarifying the cellular and molecular processes that regulate initiation and resolution of synovial inflammation is essential for advancing therapeutic strategies. This study focused on characterizing heterogeneous STM populations, particularly the MerTK$^+$CD206$^+$ subset, to define their functional roles during active and remission phases of RA and to investigate their mechanistic linkage to pathogenesis through NF-κB and JAK1/STAT3 signaling pathways.

Initial phenotyping of clinical samples by flow cytometry revealed an altered STM composition during remission. Subsets co-expressing MerTK$^+$CD206$^+$, CD163$^+$ CD206$^+$, and MerTK$^+$CD163$^+$ were present at significantly higher frequencies in synovial tissue of clinically inactive RA patients compared to those with active disease. A significant inverse correlation was noted between MerTK$^+$CD206$^+$ STM abundance and the DAS28 index. MerTK, a member of the TAM (Tyro3, Axl, MerTK) receptor tyrosine kinase family, is activated by its ligand growth arrest-specific 6 (Gas6) and modulates inflammatory and immune processes in various cells [24-26]. CD206, often used as a marker for M2-like or alternatively activated macrophages, is associated with tissue repair and inflammation resolution [27-29]. Thus, the MerTK$^+$CD206$^+$ phenotype likely identifies an STM subpopulation with anti-inflammatory and tissue-protective attributes.

Functional assessment via an *in vitro* LPS stimulation assay demonstrated a clear contrast between MerTK$^+$ CD206$^+$ and MerTK$^-$CD206$^-$ STMs. Upon stimulation, MerTK$^-$CD206$^-$ cells released large amounts of pro-inflammatory cytokines, including IL-1β, IL-6, and TNF-α. In contrast, MerTK$^+$CD206$^+$ STMs exhibited restrained pro-inflammatory cytokine production while uniquely producing RvD1. As a potent SPM, RvD1 inhibits neutrophil recruitment [30,31] and enhances efferocytosis (macrophage-mediated clearance of apoptotic cells) [32,33], thereby actively promoting inflammation resolution and supporting tissue repair [34-36]. These findings suggest that MerTK$^+$CD206$^+$ STMs are not merely resistant to activation but are functionally programmed to actively resolve inflammation, a trait that may underlie their association with remission.

Mechanistically, the distinct functional profile of MerTK$^+$CD206$^+$ STMs was linked to differential regulation of key inflammatory signaling pathways. Western blot analysis showed that after LPS exposure, phosphorylation levels of NF-κB, JAK1, and STAT3 - indicators of pathway activation - were considerably lower in MerTK$^+$CD206$^+$ cells compared to MerTK$^-$CD206$^-$ counterparts. The NF-κB pathway is a master regulator of inflammatory gene expression, and is strongly associated with chronic cytokine production and structural damage [37,38]. Similarly, the JAK/STAT pathway, particularly JAK1/STAT3, serves as a central amplifier of inflammatory signals initiated by cytokines such as IL-6 [39,40]. The attenuated activation of these pathways in MerTK$^+$CD206$^+$ STMs likely contributes to their reduced pro-inflammatory cytokine secretion and may support their pro-resolving functions.

This study has several limitations that should be acknowledged. First, this was a single-center study, which may introduce selection bias and limit the external validity of the findings. The absence of an independent external validation cohort further restricts the generalizability of the results, and multicenter studies are needed to confirm these observations. In addition, all synovial tissue samples were obtained exclusively from the knee joint; therefore, the findings cannot be directly extrapolated to other affected joints in RA. Furthermore, the healthy control group comprised patients undergoing anterior cruciate ligament reconstruction rather than in-

dividuals with completely healthy knee joints, and the relatively small sample size (n = 20) may have introduced some uncertainty in the estimation of baseline immune cell profiles. Second, all patients in the remission RA group received combination therapy with methotrexate and anti-TNF agents. Given that both methotrexate and TNF inhibitors can modulate macrophage polarization and function, it is difficult to fully disentangle the effects of disease remission itself from the influence of pharmacotherapy on the distribution and phenotype of STM subsets. Additionally, this study adopted a cross-sectional design without longitudinal follow-up; therefore, the temporal relationship between the dynamics of STM subsets and disease progression or treatment response could not be established. Third, the analysis of pathway phosphorylation only demonstrated an association with macrophage phenotypic features, and a causal relationship cannot be inferred from these correlational data. Moreover, the present study lacked functional validation experiments, including gain-of-function and loss-of-function approaches (e.g., MerTK overexpression or knockdown) and intervention with pathway-specific inhibitors. Further functional studies are required to delineate the causal regulatory axis between MerTK expression and the pro-resolving phenotype of STMs.

CONCLUSION

In summary, this study provides new evidence that the $MerTK^{+}CD206^{+}$ macrophage subpopulation expands within the synovial compartment during RA remission, and its frequency correlates inversely with clinical disease activity. Functionally, this subset exhibits a restrained pro-inflammatory response and active biosynthesis of the pro-resolving mediator RvD1. Mechanistically, this unique phenotype appears to be facilitated, at least in part, by diminished activation of the NF-κB and JAK1/STAT3 signaling pathways. These insights improve the understanding of cellular mechanisms driving inflammatory resolution in RA and provide a conceptual basis for designing future immunomodulatory therapies aimed at harnessing specific pro-resolving macrophage subsets.

Data Available:
Data are available from the corresponding author on request.

Ethics Statement:
All procedures performed in this study involving human participants were in accordance with the ethical standards of the institutional and/or national research committee and with the 1964 Helsinki Declaration and its later amendments or comparable ethical standards. The study protocol was approved by the Ethics Committee of Affiliated Hospital of Jiangnan University (Approval No. T202221). All participants provided written informed consent.

Declaration of Generative AI in Scientific Writing:
No artificial intelligence-assisted technologies were used in the production of this manuscript.

Declaration of Interest:
The authors have no conflicts of interest to declare.

References:

1. McInnes IB, Schett G. The pathogenesis of rheumatoid arthritis. N Engl J Med 2011;365(23):2205-2219. (PMID: 22150039)
2. Armstrong DJ, McCausland EM, Quinn AD, Wright GD. Obesity and cardiovascular risk factors in rheumatoid arthritis. Rheumatology (Oxford, England) 2006;45(6):782; author reply 782-3. (PMID: 16632480)
3. Naranjo A, Sokka T, Descalzo MA, et al. Cardiovascular disease in patients with rheumatoid arthritis: results from the QUEST-RA study. Arthritis Res Ther 2008;10(2):R30. (PMID: 18325087)
4. Hanlon MM, Smith CM, Canavan M, et al. Loss of synovial tissue macrophage homeostasis precedes rheumatoid arthritis clinical onset. Sci Adv 2024;10(39):eadj1252. (PMID: 39321281)
5. Smith MD. The normal synovium. Open Rheumatol J 2011;5: 100-6. (PMID: 22279508)
6. Yeo L, Adlard N, Biehl M, et al. Expression of chemokines CXCL4 and CXCL7 by synovial macrophages defines an early stage of rheumatoid arthritis. Ann Rheum Dis 2016;75(4):763-71. (PMID: 25858640)
7. Firestein GS, McInnes IB. Immunopathogenesis of Rheumatoid Arthritis. Immunity 2017;46(2):183-96. (PMID: 28228278)
8. Kurowska-Stolarska M, Alivernini S, Ballantine LE, et al. MicroRNA-155 as a proinflammatory regulator in clinical and experimental arthritis. Proc Natl Acad Sci U S A 2011;108(27):11193-8. (PMID: 21690378)
9. Alivernini S, Tolusso B, Petricca L, et al. Synovial features of patients with rheumatoid arthritis and psoriatic arthritis in clinical and ultrasound remission differ under anti-TNF therapy: a clue to interpret different chances of relapse after clinical remission? Ann Rheum Dis 2017;76(7):1228-36. (PMID: 28119289)
10. Kurowska-Stolarska M, Alivernini S. Synovial tissue macrophages: friend or foe? RMD Open 2017;3(2):e000527. (PMID: 29299338)
11. Culemann S, Grüneboom A, Nicolás-Ávila JÁ, et al. Locally renewing resident synovial macrophages provide a protective barrier for the joint. Nature 2019;572(7771):670-5. (PMID: 31391580)
12. Alivernini S, MacDonald L, Elmesmari A, et al. Distinct synovial tissue macrophage subsets regulate inflammation and remission in rheumatoid arthritis. Nat Med 2020;26(8):1295-306. (PMID: 32601335)

13. Bhatt D, Ghosh S. Regulation of the NF-κB-Mediated Transcription of Inflammatory Genes. Front Immunol 2014;5:71. (PMID: 24611065)

14. Makarov SS. NF-kappa B in rheumatoid arthritis: a pivotal regulator of inflammation, hyperplasia, and tissue destruction. Arthritis Res 2001;3(4):200-6. (PMID: 11438035)

15. Seyedi D, Espandar N, Hojatizadeh M, Mohammadi Y, Sadri F, Rezaei Z. Noncoding RNAs in rheumatoid arthritis: modulators of the NF-κB signaling pathway and therapeutic implications. Front Immunol 2024;15:1486476. (PMID: 39530095)

16. Peng X, Wang Q, Li W, et al. Comprehensive overview of microRNA function in rheumatoid arthritis. Bone Res 2023;11(1):8. (PMID: 36690624)

17. Isomäki P, Junttila I, Vidqvist KL, Korpela M, Silvennoinen O. The activity of JAK-STAT pathways in rheumatoid arthritis: constitutive activation of STAT3 correlates with interleukin 6 levels. Rheumatology (Oxford) 2015;54(6):1103-13. (PMID: 25406356)

18. Wang C, Song Y, Wang X, Mao R, Song L. Baicalin Ameliorates Collagen-Induced Arthritis Through the Suppression of Janus Kinase 1 (JAK1)/Signal Transducer and Activator of Transcription 3 (STAT3) Signaling in Mice. Med Sci Monit 2018;24:9213-22. (PMID: 30562763)

19. Zhang F, Zhang Y, Zhou J, et al. Metabolic effects of quercetin on inflammatory and autoimmune responses in rheumatoid arthritis are mediated through the inhibition of JAK1/STAT3/HIF-1α signaling. Mol Med 2024;30(1):170. (PMID: 39390367)

20. Aletaha D, Neogi T, Silman AJ, et al 2010 Rheumatoid arthritis classification criteria: an American College of Rheumatology/ European League Against Rheumatism collaborative initiative. Arthritis Rheum 2010;62(9):2569-81. (PMID: 20872595)

21. Kurowska-Stolarska M, Alivernini S. Synovial tissue macrophages in joint homeostasis, rheumatoid arthritis and disease remission. Nat Rev Rheumatol 2022;18(7):384-97. (PMID: 35672464)

22. de Molon RS, Rossa C, Jr., Thurlings RM, Cirelli JA, Koenders MI. Linkage of Periodontitis and Rheumatoid Arthritis: Current Evidence and Potential Biological Interactions. Int J Mol Sci 2019;20(18):4541. (PMID: 31540277)

23. Lewis MJ. Predicting best treatment in rheumatoid arthritis. Semin Arthritis Rheum 2024;64s:152329. (PMID: 38008706)

24. Liu SY, Yeh YJ, Xue TY, et al. Hydroxychloroquine enhances efferocytosis and modulates inflammation via MerTK/Gas6 signaling in a pristane-induced lupus mouse model. Front Immunol 2025;16:1524315. (PMID: 40589760)

25. Di YX, Bao YJ, Zhu ZQ, et al. Tomentosin suppressed M1 polarization via increasing MERTK activation mediated by regulation of GAS6. J Ethnopharmacol 2023;314:116429. (PMID: 37011736)

26. Lahey KC, Gadiyar V, Hill A, et al. Mertk: An emerging target in cancer biology and immuno-oncology. Int Rev Cell Mol Biol 2022;368:35-59. (PMID: 35636929)

27. Chen F, Wang N, Liao J, et al. Esculetin rebalances M1/M2 macrophage polarization to treat sepsis-induced acute lung injury through regulating metabolic reprogramming. J Cell Mol Med 2024;28(21):e70178. (PMID: 39535339)

28. Liang CL, Jiang H, Feng W, et al. Total Glucosides of Paeony Ameliorate Pristane-Induced Lupus Nephritis by Inducing PD-l ligands(+) Macrophages via Activating IL-4/STAT6/PD-L2 Signaling. Front Immunol 2021;12:683249. (PMID: 34290705)

29. Ma S, He H, Ren X, et al. Luteolin ameliorates periodontitis by modulating mitochondrial dynamics and macrophage polarization via the JAK2/STAT3 pathway. Int Immunopharmacol 2025;144: 113612. (PMID: 39579538)

30. Li W, Shepherd HM, Terada Y, et al. Resolvin D1 prevents injurious neutrophil swarming in transplanted lungs. Proc Natl Acad Sci U S A 2023;120(31):e2302938120. (PMID: 37487095)

31. Li L, Cheng SQ, Sun YQ, et al. Resolvin D1 reprograms energy metabolism to promote microglia to phagocytize neutrophils after ischemic stroke. Cell Rep 2023;42(6):112617. (PMID: 37285269)

32. Hosseini Z, Marinello M, Decker C, et al. Resolvin D1 Enhances Necroptotic Cell Clearance Through Promoting Macrophage Fatty Acid Oxidation and Oxidative Phosphorylation. Arterioscler Thromb Vasc Biol 2021;41(3):1062-75. (PMID: 33472399)

33. Gerlach BD, Marinello M, Heinz J, et al. Resolvin D1 promotes the targeting and clearance of necroptotic cells. Cell Death Differ 2020;27(2):525-39. (PMID: 31222041)

34. Hsiao HM, Thatcher TH, Colas RA, Serhan CN, Phipps RP, Sime PJ. Resolvin D1 Reduces Emphysema and Chronic Inflammation. Am J Pathol 2015;185(12):3189-201. (PMID: 26468975)

35. Petrillo F, Trotta MC, Bucolo C, et al. Resolvin D1 attenuates the inflammatory process in mouse model of LPS-induced keratitis. J Cell Mol Med 2020;24(21):12298-307. (PMID: 33058526)

36. Hardesty JE, Warner JB, Song YL, et al. Resolvin D1 attenuated liver injury caused by chronic ethanol and acute LPS challenge in mice. FASEB J 2023;37(1):e22705. (PMID: 36520060)

37. Ilchovska DD, Barrow DM. An Overview of the NF-kB mechanism of pathophysiology in rheumatoid arthritis, investigation of the NF-kB ligand RANKL and related nutritional interventions. Autoimmun Rev 2021;20(2):102741. (PMID: 33340772)

38. Li J, Tang RS, Shi Z, Li JQ. Nuclear factor-κB in rheumatoid arthritis. Int J Rheum Dis 2020;23(12):1627-35. (PMID: 32965792)

39. Hu L, Liu R, Zhang L. Advance in bone destruction participated by JAK/STAT in rheumatoid arthritis and therapeutic effect of JAK/STAT inhibitors. Int Immunopharmacol 2022;111:109095. (PMID: 35926270)

40. Srivastava S, Samarpita S, Ganesan R, Rasool M. CYT387 Inhibits the Hyperproliferative Potential of Fibroblast-like Synoviocytes via Modulation of IL-6/JAK1/STAT3 Signaling in Rheumatoid Arthritis. Immunol Invest 2022;51(6):1582-97. (PMID: 34704880)